npj | Computational Materials

www.nature.com/npjcompumats

ARTICLE OPEN

Sequential slip transfer of mixed-character dislocations across Σ3 coherent twin boundary in FCC metals: a concurrent atomistic-continuum study

Shuozhi Xu[1], Liming Xiong[2], Youping Chen[3] and David L McDowell[1,4]

Sequential slip transfer across grain boundaries (GB) has an important role in size-dependent propagation of plastic deformation in polycrystalline metals. For example, the Hall–Petch effect, which states that a smaller average grain size results in a higher yield stress, can be rationalised in terms of dislocation pile-ups against GBs. In spite of extensive studies in modelling individual phases and grains using atomistic simulations, well-accepted criteria of slip transfer across GBs are still lacking, as well as models of predicting irreversible GB structure evolution. Slip transfer is inherently multiscale since both the atomic structure of the boundary and the long-range fields of the dislocation pile-up come into play. In this work, concurrent atomistic-continuum simulations are performed to study sequential slip transfer of a series of curved dislocations from a given pile-up on Σ3 coherent twin boundary (CTB) in Cu and Al, with dominant leading screw character at the site of interaction. A Frank-Read source is employed to nucleate dislocations continuously. It is found that subject to a shear stress of 1.2 GPa, screw dislocations transfer into the twinned grain in Cu, but glide on the twin boundary plane in Al. Moreover, four dislocation/CTB interaction modes are identified in Al, which are affected by (1) applied shear stress, (2) dislocation line length, and (3) dislocation line curvature. Our results elucidate the discrepancies between atomistic simulations and experimental observations of dislocation-GB reactions and highlight the importance of directly modeling sequential dislocation slip transfer reactions using fully 3D models.

npj Computational Materials (2016) **2,** 15016; doi:10.1038/npjcompumats.2015.16; published online 29 January 2016

INTRODUCTION

The strength of polycrystalline face-centered cubic (FCC) metals varies characteristically with the average grain size.[1] For grain size above 10 nm, the Hall–Petch effect that a smaller average grain size results in a higher yield stress, is confirmed by experiments,[2] constitutive modelling,[3] and atomistic simulations.[4] For a FCC polycrystal with sufficiently large grains and few short-range dislocation interactions (e.g., during stage I work hardening), the Hall–Petch effect can be rationalised in terms of the dislocation pile-up model.[1] Since the stress on the leading dislocation is proportional to the applied stress and to the number of dislocations in the pile-up, the tip of the pile-up in a smaller grain that accommodates fewer dislocations experiences a lower stress.[5] Thus, a higher applied stress is required to reach the critical stress level on the incoming side of the grain boundary (GB) to activate dislocation motion on the other side. Generally referred to as slip transfer processes, four possible lattice dislocation/GB reactions have been identified: direct transmission of the incoming dislocation, absorption of the incoming dislocation into an extrinsic GB dislocation, desorption of the GB dislocation into a neighbouring grain, and reflection back into the original grain.[6] At low levels of plastic strain, plastic deformation within individual grains is mainly carried by multiplication/generation of lattice dislocations, the resistance to which is manifested as the strength of polycrystal.[7] For polycrystalline metals with an average grain size above 100 nm or so, strength is mainly controlled by the generation of lattice dislocations. Thus, dislocation pile-ups and associated slip transfer at GBs have an important role in size dependent initiation and propagation of plastic deformation in polycrystalline metals.[7] At large plastic strain, however, significant dislocation network density dominates the work hardening; dislocation multiplication is restricted, pile-up is relaxed, and the dependence of strength on grain size then diminishes relative to the dependence on the dislocation substructure scale(s).[1]

On the basis of experimental observations, Lee *et al.*[6] formulated the Lee–Robertson–Birnbaum (LRB) slip transfer criteria, which take into account geometry, resolved shear stress and residual GB dislocations. In recent years, a series of *in situ* transmission electron microscopy (TEM) studies have been conducted in sequential slip transfer through GBs/interphase boundaries in FCC metals, hexagonal close-packed (HCP) metals and body-centered cubic (BCC) metals containing a variety of dislocations and boundaries with the influence of impurities or irradiation at different strain rate/temperature.[8] While the local stress is considered to be important for slip transfer, other factors including dislocation/GB types, lattice orientation, loading direction, dislocation impingement sites and the nature of neighboring grains can also be influential.[8] For a symmetric Σ3 coherent twin boundary (CTB) on a {111} plane, screw dislocation pile-ups can either cross slip onto a plane close and parallel to the twin plane or be absorbed by the CTB before being emitted into the twinned

[1]Woodruff School of Mechanical Engineering, Georgia Institute of Technology, Atlanta, GA, USA; [2]Department of Aerospace Engineering, Iowa State University, Ames, IA, USA; [3]Department of Mechanical and Aerospace Engineering, University of Florida, Gainesville, FL, USA and [4]School of Materials Science and Engineering, Georgia Institute of Technology, Atlanta, GA, USA.
Correspondence: DL McDowell (david.mcdowell@me.gatech.edu)
Received 18 July 2015; revised 13 December 2015; accepted 15 December 2015

grain.[9] In this work, we focus on a Σ3 CTB because that it is a dominant feature in twinned FCC metals and manifests excellent mechanical properties;[10] moreover, it is among the most prevalent GBs in FCC polycrystals.[1]

Atomistic simulations have been performed to quantify dislocation/GB reactions.[9–14] Such simulations have found that in FCC pure metals, a screw dislocation can either directly transmit through the CTB by the Fleischer (FL) mechanism,[10,11] be absorbed and then desorbed into the twinned grain by the Friedel–Escaig (FE) mechanism,[10–12] or glide on the twin boundary plane.[12] The process that controls the reaction mechanism is subject to debate.[9] Ezaz *et al.*[14] proposed that the energy barrier in slip-CTB interaction is proportional to the magnitude of the Burgers vector of the residual dislocation, with the screw dislocation directly transmitting through the CTB and non-screw dislocations leaving a residual dislocation on the CTB, which then elevates the local stress and energy barrier for further dislocation transmission. Using the climbing image nudged elastic band (CINEB) method, Zhu *et al.*[10] found for Cu that at low applied stress, the activation energy for absorption is lower than that for direct transmission, the latter of which temporarily leaves a stair-rod dislocation on the CTB; further, the desorption energy barrier is much higher because two TB Shockley partials which were widely separated during absorption need to be constricted. Chassagne *et al.*[9] showed that there exists a critical reaction stress below which the screw dislocation glides on the CTB and above which the dislocation is absorbed and then desorbed into the nanotwin. In their study and that of Jin *et al.*,[12] no FL type direct transmission of screw dislocation through a CTB was observed.

However, typical atomistic simulations employ only an isolated, short, straight dislocation segment associated with a periodic image in a quasi 2D specimen,[9,12,13] or situate the source very near the interface with a very limited volume of a periodic unit cell.[14] In such cases of confined volumes and highly constrained simulation cell, image forces originating from the interaction between periodic or non-periodic boundaries and dislocations are typically non-negligible.[15–17] In some atomistic simulations,[18] a short crack in adjacent to GB is introduced to nucleate a 3D dislocation network which, like an indenter or a void, is not suitable for our work where a series of dislocations in a single pile-up is desired over extended distances. Moreover, experiments show that the slip transfer with an increasing number of incoming dislocations can activate additional slip systems or alter the dislocation emission.[8] It is therefore difficult to use results obtained for a single dislocation/GB interaction to extrapolate to the practical case of sequential slip transfer of multiple dislocations in a pile-up.

A commonly stated goal to enhance dislocation-based continuum modelling of polycrystals is to include effects of sequential slip transfer. Such models include the crystal plasticity finite element method (CPFEM),[19] the discrete dislocation dynamics (DDD),[20] the field dislocation mechanics[21] and the phase field method.[22] However, these continuum models do not naturally incorporate the necessary degrees of freedom associated with the GBs and other evolving internal state variables that relate to slip-transfer critieria.[23] In CPFEM, for example, a core-mantle type of approach can be employed where, compared with dislocation motion in grain interior, the slip transfer overcomes either a higher energy barrier, a larger slip resistance, a higher work hardening rate or a high dislocation density region.[19] Moreover, details of the dislocation structure, including stacking fault and core structures that affect GB slip transfer,[9,12] are not explicitly addressed in CPFEM or other continuum approaches such as DDD. While DDD updates the positions and velocities of all dislocation segments at each instant and tracks the long-range elastic interactions of dislocations, the short-range dislocation interaction follows prescribed rules.[20] Further, in DDD, high-angle GBs are typically avoided, considered as impenetrable obstacles, or the stress field at the leading dislocation in the pile-up activates dislocation sources that are embedded either at GBs or in the neighbouring grain. Low-angle GBs are described by arrays of dislocations.[24] DDD largely ignores the role of GBs as dislocation sources even in the absence of pile-ups, as well as GB sliding/migration and elastic anisotropy.[25] For these reasons, atomistic simulations are preferred to understand GB structure-specific slip-transfer responses.

The sequential slip transfer process in a dislocation pile-up bypass of GBs is inherently multiscale; the GB structure evolution requires explicit atomistic treatment, whereas the dislocation pile-up itself has long-range character.[25] In this spirit, multiscale modelling has been pursued using the quasicontinuum (QC) method[26] and the coupled atomistic and discrete dislocation (CADD) method[27] to investigate sequential slip transfer. Although simulations following both methods employed a sufficiently large continuum domain to incorporate long-range fields of dislocation pile-ups and an atomistic domain for representation of GBs, to our knowledge this work has considered either quasi 2D approximations for segments or periodic boundary conditions (PBCs) along the dislocation line direction. In these models, (1) curved dislocations of mixed character have been excluded because of the 2D setup and (2) both ends of the outgoing dislocation line are forced to be 'reconnected' across the periodic boundary, effectively changing the length and forcing unrealistic constriction events. Moreover, the continuum domain in the QC approach associated with local nodes does not admit dislocations, so the finite elements must be adaptively remeshed to full atomistic resolution along the slip propagation path, even well away from interfaces; glide dislocations nucleated from either nanoindentation or a crack tip must pass through a fully resolved atomistic domain, which is relatively small due to its high computational cost and the corresponding dislocation density is much higher than that in experiments. The 2D CADD method adopts a 'detection band' to transfer dislocations between atomistic and continuum domains, yet a full 3D coupling of atomistic and discrete dislocation methods allowing curved dislocations has not yet been achieved or is in early stages of consideration.[28]

Therefore, we turn our attention to approaches which (1) describe interface reactions using fully resolved atomistics, (2) preserve the net Burgers vector and associated long-range stress fields of curved, mixed-character dislocations in a sufficiently large continuum domain in a fully 3D model, and preferably, (3) employ the same governing equations and interatomic potentials in both domains to avoid the usage of phenomenological parameters, essential remeshing operations or criteria and *ad hoc* procedures for passing dislocation segments between atomistic and coarse-grained atomistic domains. One such approach is the concurrent atomistic-continuum (CAC) method, a coarse-grained finite element integral formulation for the balance equations that admits propagation of displacement discontinuities (dislocations) through a lattice while employing only the underlying interatomic potential as a constitutive relation. Building on the foundation of a unified atomistic-continuum formulation,[29] CAC simulations admit descriptions of dislocations and stacking faults without adaptive refinement in the coarse-grained domain; the displacement fields of line/planar defects (e.g., Burgers vector) are smeared at interelement discontinuities. Both quasistatic[30] and dynamic CAC[31] have demonstrated capabilities to reproduce complex dislocation phenomena in FCC metals such as curved dislocation loop nucleation/migration and dislocation-void interactions.[32] Using nonlocality and an accurate representation of generalised stacking fault energy in both atomistic and coarse-grained domains, dislocations can pass through the domain interface smoothly without ghost forces or the need of overlapping pad regions.[30] The success of these calculations suggests the viability of using

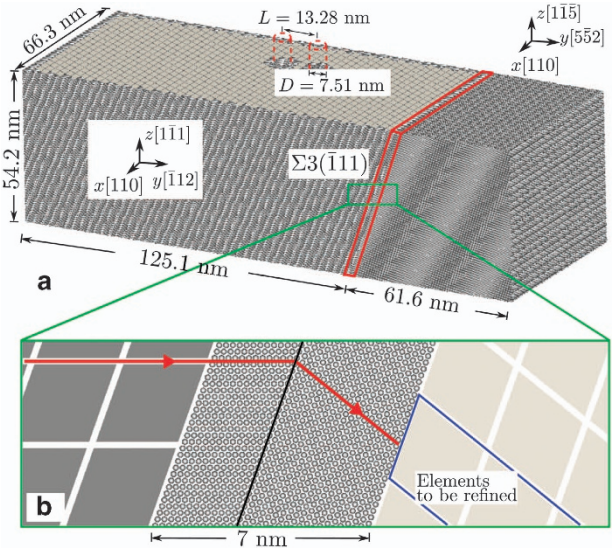

Figure 1. (**a**) Bicrystal simulation cell to study sequential slip across a Σ3 CTB in FCC metals. A pair of cylindrical holes is introduced as an FR source for dislocation multiplication. An atomistic domain is meshed in the vicinity of CTB, FR source, and at the otherwise zigzag boundaries; away from the CTB, holes, and boundaries are those of the coarse-grained finite elements, each of which contains 2,197 atoms. All boundaries are assumed stress free to allow full 3D description. (**b**) A zoom-in of the CTB region shows that the elements marked by the blue lines need to be refined for outgoing dislocations to propagate as they exit the atomistically resolved domain of the CTB. Note that all distances labelled here are for Cu; the size of the model for Al differs by the ratio of their lattice parameters.

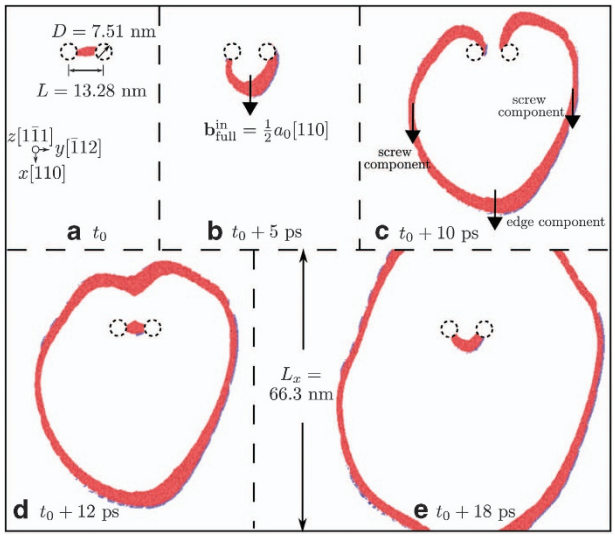

Figure 2. Snapshots of dislocation loop multiplication in Cu subject to the applied shear stress σ_{xz} between a pair of cylindrical holes, which serve as an FR source. Atoms are colored by adaptive common neighbor analysis:[49] red are of HCP local structure, blue are not coordinated as either FCC or HCP, and all FCC atoms are deleted. In **a**, a straight edge dislocation is introduced between two cylindrical holes. In **b**, the dislocation reaches the critical semi-elliptical configuration; then it continues growing in **c** until a dislocation loop is formed in **d**. In **e**, the segments of dislocation loop with edge component are swept out at the stress-free boundaries, leaving a curved dislocation moving along the positive *y* direction towards the CTB. Similar phenomena are observed for Al.

CAC simulations in the context of sequential slip transfer across GBs in FCC metals.

In this paper, we perform CAC simulations for Cu and Al to clarify the mechanisms of the interactions between a number of curved incoming dislocations in a single pile-up and a Σ3 CTB, to our knowledge the first attempt to do so in the literature. Dewald and Curtin[27] conducted simulations of straight pure screw dislocation segments with a Σ3 CTB for Al using the CADD method, and had elucidated several additional criteria for slip transfer beyond those of the classical LRB criteria;[6] however, we are interested in exploring whether the findings of that kind of quasi-2D study hold up for cases of larger scale full 3D simulations of sequential dislocation slip transfer reactions, which prevail in *in situ* TEM experiments.[33] The differences between experimental and computational studies are analysed. These two FCC systems are selected based on the works of Chassagne *et al.*[9] and Jin *et al.*[12,13] as they have significantly different stable/unstable stacking/twin fault energies that affect the slip transfer reactions; moreover, they have planar dislocation cores,[34] which can be well accommodated along interelement boundaries in CAC. Dislocation reactions upon transmission and the corresponding CTB structure evolution will be investigated for a sequence of reactions of successive dislocations in a pile-up. We explore three scientific questions:

(1) How do the interactions of curved, mixed character dislocations with the CTB in a full 3D simulation differ from those of straight dislocation/CTB interactions in a quasi 2D simulation cell?
(2) How does the dislocation/CTB reaction change subject to different applied shear stress, dislocation line length, and dislocation line curvature?
(3) How do initial slip transfer events influence subsequent interactions of pile-up dislocations with the CTB?

While large-scale atomistic simulations are desirable in studying slip transfer across GBs, our purpose in this paper is to demonstrate the efficacy of coarse-graining in facilitating parametric studies of dislocation/GB reactions concerning a wide range of dislocations and GBs for the same computational resources. It is anticipated that this kind of coarse-grained modelling may assist in formulating constitutive laws and rules in describing slip transfer that may be useful upstream in DDD and CPFEM simulations.

RESULTS

The bicrystal simulation cell containing a Σ3 CTB is shown in Figure 1, with a pair of cylindrical holes introduced in the incoming grain throughout the specimen along the *z* direction. Full atomistic resolution is applied within 7 nm in the vicinity of CTB, around the holes, and at the otherwise zigzag boundaries;[30] away from the CTB, holes, and boundaries are the interfaces of discontinuous elements. The cylindrical holes effectively serve as a Frank–Read (FR) source to generate a series of curved dislocations in a single-ended pile-up as they are shown to strongly pin dislocations in FCC metals in the presence of stress-free boundaries.[35] Such a simulation cell is introduced because we are interested in promoting a full 3D effect and modeling specimen thicknesses that are comparable to those of TEM foils to facilitate more direct comparison with *in situ* TEM experiments. Effects of free surfaces on dislocation curvature are of interest; to the best of our knowledge, these effects have not been pursued in prior atomistic simulations. Details of the simulations are supplied in Materials and Methods.

In both Cu and Al, the initially straight edge dislocation segment that was anchored at two cylindrical holes in the absence of external stress responds to application of the shear stress σ_{xz} by

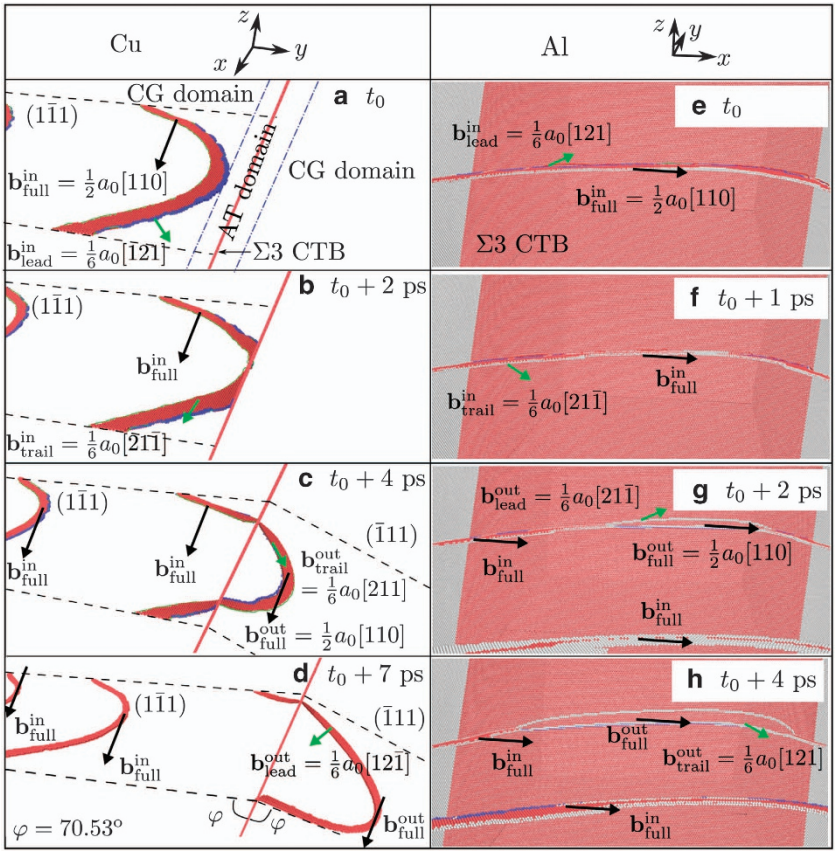

Figure 3. Snapshots of dislocation pile-up impingement with dominant leading screw character against Σ3 CTB in both Cu (**a**–**d**) and Al (**e**–**h**). Atoms are colored in the same way as in Figure 2. A fully atomistic domain is meshed in the vicinity of the CTB, as shown in **a**. In both materials, the incoming dislocation is constricted at the CTB, where two 30° Shockley partial dislocations are recombined into a full dislocation. In Cu, the dislocation cuts into the outgoing twinned grain and is redissociated into two partials; in Al, the redissociated dislocation is absorbed by the CTB, with two partials gliding on the twin plane in the same direction. Different views of the CTB are taken for Cu and Al, which are illustrated in the first row of each column.

bowing out, as shown in Figure 2. In Figure 2b, the critical configuration of a semi-ellipse is reached; then the segment continues growing until two parts contact and annihilate each other, as shown in Figure 2c. In Figure 2d, a dislocation loop is formed, leaving a straight edge dislocation segment behind as the new FR source. The segment of the dislocation loop with edge component has a wider core than that with screw component, consistent with both elasticity theory[5] and atomistic simulations.[36] As the dislocation loop continues to expand, the segment with edge component exits at the stress-free surface, leaving a screw dislocation dipole in the incoming grain, as shown in Figure 2e. Subject to a shear stress σ_{xz}, one curved dislocation segment moves towards the CTB, whereas the other eventually exits at the leftmost stress-free boundary.

In both materials, the core of the dislocation is split into two 30° Shockley partial dislocations, i.e.,

$$\frac{1}{2}a_0[110]^{\text{in}} \rightarrow \frac{1}{6}a_0[121]^{\text{in}}_{\text{lead}} + \frac{1}{6}a_0[21\bar{1}]^{\text{in}}_{\text{trail}} \quad (1)$$

Here and throughout the remainder of this paper, the superscripts 'in' and 'out' are used to distinguish the two grains in which the dislocation is located, whereas the subscripts 'lead' and 'trail' refer to leading and trailing partial dislocations, respectively. The reaction is energetically favourable according to Frank's rule.[5] In the coarse-grained domain, the two partials are separated by 29 and 19 Å in Cu (Figure 3a) and Al (Figure 3e), respectively, somewhat wider than separations computed using full atomistic simulations. Once the dislocation migrates into the atomistic domain in the vicinity of the CTB, it obtains the same stacking fault width and core structure as those from full atomistics[30] and feels a repulsive force from the CTB in Cu but an attractive force in Al because of the relatively low CTB shear strength in Al.[37] At a shear stress of 1.2 GPa, two dislocation-CTB interaction modes are found:

In Cu, the leading partial in the incoming grain is stopped at the CTB, with the stacking fault width constricting up to the point where the trailing partial also reaches the CTB, as shown in Figure 3b. Then the full dislocation is redissociated into two 30° Shockley partials and transmitted into the outgoing grain, i.e.,

$$R\cdot\frac{1}{2}a_0[110]^{\text{in}} \rightarrow \frac{1}{2}a_0[110]^{\text{out}} \rightarrow \frac{1}{6}a_0[12\bar{1}]^{\text{out}}_{\text{lead}} + \frac{1}{6}a_0[211]^{\text{out}}_{\text{trail}} \quad (2)$$

Here the slip plane in the outgoing grain is $(\bar{1}11)$ and the rotation matrix between two grains is

$$R = \frac{1}{3}\begin{pmatrix} 1 & 2 & 2 \\ 2 & 1 & -2 \\ -2 & 2 & -1 \end{pmatrix} \quad (3)$$

In Al, the leading and trailing partial dislocations are spontaneously absorbed by and constricted at the CTB because of the attractive force. However, instead of transmitting into the outgoing grain, the full dislocation is re-dissociated to two 30° Shockley partials in the twin plane, i.e.,

$$R\cdot\frac{1}{2}a_0[110]^{\text{in}} \rightarrow \frac{1}{2}a_0[110]^{\text{out}} \rightarrow \frac{1}{6}a_0[21\bar{1}]^{\text{out}}_{\text{lead}} + \frac{1}{6}a_0[121]^{\text{out}}_{\text{trail}} \quad (4)$$

where the slip plane (i.e., twin plane) for the outgoing grain is $(1\bar{1}1)$.

In both materials, up to three dislocation loops are nucleated from the FR source and sequentially interact with the CTB. Each time a dislocation loop is generated, the cylindrical holes acquire steps at the free surface that potentially affects the source behavior; however, this is not of significant concern here as our intent is only to introduce successive dislocations on the same slip plane. Driven by the shear stress, the first dislocation migrates toward the CTB but stops at a distance when the applied shear stress, dislocation self force, repulsive force from the CTB, and the force required to create surface steps are balanced during energy minimisation. In the subsequent quenched dynamics, the second dislocation loop is formed, which drives the first dislocation towards the CTB. The CTB structure is found by energy minimisation. The last dislocation is nucleated from the FR source after the first but before the second dislocation/CTB interaction occurs. As more dislocation loops are formed, the FR source becomes progressively exhausted for a given applied stress as dislocations interact with upstream dislocations in the pile-up.

To better understand the geometric conditions involved in our simulations and compare our results with quasi 2D simulations and *in situ* TEM experiments in the literature, we also studied cases of different applied shear stresses, dislocation line length, and dislocation line curvature.

DISCUSSION

The critical stress for an edge dislocation bow-out between two cylindrical holes can be estimated by Scattergood–Bacon equation,[38] which considers the image force on dislocations due to the hole surface and is confirmed by atomistic simulation[39] to accurately predict the critical stress at the nanometer scale, i.e.,

$$\tau_c = \frac{\mu b}{2\pi(L-D)}\left[\ln\left(\frac{r_0}{D}+\frac{r_0}{L-D}\right)^{-1}+1.52\right] \quad (5)$$

where μ is the shear modulus for $[110]\langle 1\bar{1}1\rangle$ slip system, L the distance between the centers of two cylindrical holes, D the diameter of each hole, and r_0 the dislocation core radius. If we set r_0 to b, equation (5) gives $\tau_c = 1.18$ GPa for Cu and 803 MPa for Al. In our simulations, after generating the first dislocation, the applied stress is ramped to and maintained at 1.2 GPa for both materials to bow out subsequent dislocations from the FR source and drive curved dislocations towards the CTB. The image forces on a dislocation with dominant screw character caused by stress-free boundaries, which are naturally captured in CAC via nonlocal, nonlinear interatomic force instead of by superposition via linear elastic solutions as in DDD,[17] are much smaller than those on edge and mixed type dislocations.[36] Particularly for the top and bottom surfaces, the image forces are negligible because the Burgers vector is parallel to these boundaries.[36]

Our CAC simulations suggest that for both Cu and Al, the dissociated dislocations in the incoming grain are constricted into a full dislocation at the CTB. This is because the arrangement of the leading and trailing dislocations must be switched before either entering the outgoing grain or gliding on the twin plane. Using a dislocation extraction algorithm (DXA),[40] we find that the reaction of dislocation at the CTB in terms of the transformed Burgers vector is

$$[1.28, 0.74, 0]^{\text{in}}_{\text{lead}} + [1.28, -0.74, 0]^{\text{in}}_{\text{trail}} \rightarrow [1.28, -0.32, 0.54]^{\text{out}}_{\text{lead}} + [1.28, 0.32, -0.54]^{\text{out}}_{\text{trail}} \quad (6)$$

for Cu, and

$$[1.43, 0.83, 0]^{\text{in}}_{\text{lead}} + [1.43, -0.83, 0]^{\text{in}}_{\text{trail}} \rightarrow [1.43, -0.26, 0.65]^{\text{out}}_{\text{lead}} + [1.43, -0.26, -0.65]^{\text{out}}_{\text{trail}} \quad (7)$$

for Al. Equations (6) and (7) show that for at least one of the incoming partials, the y component of the transformed Burgers vector, i.e., the pure edge component, changes sign, a process not possible without recombination and redissociation since no stair-rod dislocation (as in the FL mechanism) is observed at the CTB. This requirement of two partial dislocations to exchange their order at the CTB is attributed to the twin symmetry.[12,13] Particularly for a 3D curved dislocation, part of the segment with pure screw component is constricted first, leaving the dissociated segment with mixed type component behind in the incoming grain, as shown in Figures 3c,g. This phenomenon, similar to the twinning dislocation multiplication at a CTB,[16] cannot be described using quasi 2D simulations but is reported in experiments.[8]

For Cu, the leading dislocation does not penetrate into the outgoing grain when the trailing partial is still in the incoming grain; the direct transmission of dislocations by the FL mechanism is not observed. In our simulation, the dislocation reaction is of FE type, i.e., the dissociated dislocation is always recombined at the CTB before any further motion can proceed, a phenomenon supported by atomistic simulations.[9,12] Interestingly, we did not find any CTB dislocations in the process of dislocation constriction, while NEB[10] predicts that the dislocations are absorbed to form CTB dislocations followed by desorption. We note that molecular statics is used by practitioners of NEB to determine initial and final replicates and molecular dynamics (MD) is sometimes employed to explore candidate transition states between these two replicates, before the 0 K energy minimised NEB method is used to identify the correct saddle point on the minimum-energy pathway. In the case of extended defects with complex reactions, this can be problematic when using overdriven dynamics of MD since the pathway taken in such simulations may be away from the near equilibrium trajectory associated with thermally activated, low-stress regime. After the first dislocation passes the CTB, the elements with edges along the blue lines in Figure 1 are refined, because the outgoing dislocation path is not aligned with the interelement boundaries and it would therefore be impeded, requiring cross-slip along the atomistic/coarse-grained interface and posing an aphysical back stress acting on subsequent dislocation reactions. The outgoing dislocation then continues migrating on the $(\bar{1}11)$ plane until it exits the rightmost stress-free boundary.

For Al, the incoming dislocation is always spontaneously absorbed and constricted by the CTB. After recombination, the full dislocation is split onto the CTB instead of passing it because of its relatively higher stable stacking fault energies.[9,12] In other words, the screw dislocation cross-slips on the CTB following the FE mechanism. The 30° CTB partials, with Burgers vectors parallel to the CTB, belong to the displacement shift complete lattice for the CTB and therefore migrate freely in the same direction. Our result differs from those obtained using quasi 2D atomistic[9,12] and multiscale simulations via the CADD method,[27] where two CTB partials move in opposite directions, adding one layer of atoms to the outgoing grain at the expense of the incoming grain, a process termed detwinning. In our simulation, only a local detwinning process that grows the incoming grain is temporarily observed; the CTB remains perfect after both partials glide to and are eventually swept out at the top stress-free boundary.

The different dislocation reactions at the CTB for Cu and Al under the same applied stress may relate to the fact that the normalised Hall–Petch coefficient for Cu is about twice that for Al.[1] For both materials, since each dislocation-CTB slip transfer event does not leave residual Burgers vector in the CTB interface, the interaction mechanism for subsequent dislocations is found to be precisely the same as for the first dislocation for each same material. We emphasise that this finding is particular to the Σ3 CTB and to the nature of the incoming dislocations considered here.

To further explore the differences between our simulations and those in the literature, we vary the applied stress from 100 MPa up to 2.4 GPa for Al, with an increment of 100 MPa. Note that a shear stress lower than 803 MPa is reached using the Parrinello–Rahman

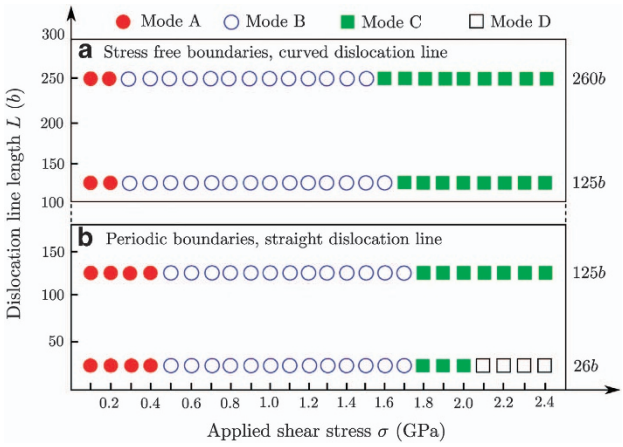

Figure 4. Four different dislocation-CTB reaction modes for Al, as a function of applied shear stress, dislocation line length, and dislocation line curvature. Prior atomistic simulations and multiscale methods in the literature only reported mode A reaction while other modes are observed in *in situ* TEM experiments. The surface steps at the stress-free boundaries in **a** retain curved dislocations while the PBCs applied on the dislocation line direction in **b** result in straight dislocation segments, regardless of the dislocation line length.

(PR) approach after each dislocation loop is emitted from the source at a higher stress, past the saddle point of the transition. With a Peierls stress of about 16 MPa[36] for a screw dislocation in Al, the stress levels employed in our simulations are high enough to retain a curved dislocation induced by the surface steps at stress-free boundaries. To study the influence of dislocation line length which is 125*b* shown in Figure 1, we investigate models with smaller dislocation line lengths L_x of 125*b* and 26*b*, respectively, where *b* is the magnitude of Burgers vector of a full dislocation. Since 26*b* is too small to accommodate the FR source, we introduce three screw dislocations spaced 50 nm from each other on the mid plane normal to *z* axis via a Volterra displacement followed by energy minimisation. For $L_x = 125b$, we also study the effect of dislocation line curvature, which is adjusted by varying the boundary conditions along the dislocation line direction: applying PBCs and stress-free boundary conditions result in a straight and a curved dislocation line, respectively.

It is found that four dislocation-CTB interaction modes exist for Al, which relate to applied shear stress, dislocation line length, and dislocation line curvature, as shown in Figure 4. The detailed stress-dependent dislocation-CTB reactions in the case of $L_x = 26b$ are shown in Figure 5, which agree with the equivalent fully atomistic simulations with a combined quenched dynamics and quasistatic periodic energy minimisation scheme. In mode A, a screw dislocation is first absorbed by the CTB subject to 100 MPa applied stress, then the two CTB partials move in opposite directions, migrating the CTB and growing the outgoing grain, as shown in Figure 5b. This mode is reported in both atomistic[9,12] and multiscale simulations,[26] but is not observed using *in situ* TEM to the best of our knowledge. At a higher stress of 500 MPa, the screw dislocation cross-slips onto the CTB via the FE mechanism, forming two CTB partials that move in the same direction, as shown in Figure 5c. This interaction result, referred to as mode B, has been reported in a high resolution TEM experiment.[41] When the applied stress increases to 1.8 and 2.1 GPa, dislocations are desorbed by the CTB into either the outgoing or both grains, referred to as modes C and D, respectively, as shown in Figures 5d,e. The penetration of a curved dislocation across a CTB in Al is observed in *in situ* TEM experiments in the presence of a large dislocation pile-up.[33] Note that for all four modes, the incoming dislocations are recombined before being redissociated at the CTB. The stress dependence of the dislocation/GB reaction agrees with atomistic[9,12] and QC simulations,[26] as well as *in situ* TEM experiments.[8]

For the same dislocation line length of 125*b* at a shear stress of 300 or 400 MPa, the reaction of a quasi 2D straight dislocation segment at the CTB follows mode A, whereas the 3D curved dislocation line interacts with the CTB via mode B. Although our simulations consider all contributions to energy change, including surface steps at the stress-free boundaries, it is not the surface steps but the dislocation line curvature that leads to different reaction modes, because the surface steps are far from the center of the dislocation line where the dislocation/CTB interaction is locally initiated. In quasi 2D, the dislocation only has pure screw component along its straight segment; in a fully 3D model, an initially curved dislocation first encounters the CTB with dominant leading screw character, whereas the remainder of the dislocation line is of mixed type. This dislocation line curvature dependence of the dislocation/CTB reaction has not been previously reported in the literature to the best of our knowledge.

With the same boundary conditions, dislocations with different line lengths interact with the CTB differently. In quasi 2D, the mode D reaction is only observed for $L_x = 26b$ but not for $L_x = 125b$. In a 3D model at a shear stress of 1.6 GPa, dislocations with a line length of 125*b* and 260*b* lead to mode B and C reactions with the CTB, respectively. Previous NEB calculations in Al show that a screw dislocation segment shorter than 22*b* cross-slips via the FL mechanism, whereas a segment longer than 22*b* cross-slips via the FE mechanism.[42] The dislocation line length dependence of the dislocation/CTB reaction can be attributed to the energetics of dislocation constriction and dissociation, which are length dependent. Similarly, constraints on the twin boundary length also affect the type of dissociation/absorption events that are possible. This is an important result, as it indicates limitations on veracity of computed results for slip transfer using quasi 2D simulations in which the incoming straight dislocation line is of pure screw character in confined volumes. We remark that in reality the probability of such an encounter is exceedingly low.

There are four possible reasons why atomistic[9,12] and multiscale simulations based on CADD,[27] either involving a single dislocation or dislocation pile-up, predict only mode A interaction, but not other modes that are observed in *in situ* TEM experiments. The first reason is the accuracy of interatomic potential. Refs 12 and 27 use Mishin's embedded atom method (EAM) potential[43] and Ercolessi-Adams EAM potential,[44] respectively, whereas ref 9 shows that both EAM potentials predict the same interaction mode. The second reason is the stress level; in ref. 12 a 100 MPa shear stress is applied, whereas in refs 9 and 27 no external shear stress is applied, and the screw dislocation moves towards the CTB because the attractive stress between them overcomes the Peierls stress. On the other hand, while it is difficult to measure local stress in TEM experiments,[8] it is expected that the stress level at the tip of the pile-up is much higher than 100 MPa because a large number of dislocations exist in a pile-up. The third reason is the atomic scale CTB structure: both TEM experiments[9] and MD simulations[45] show that a defected CTB responds differently from a perfect one. The last possible reason is the boundary condition. In most atomistic and multiscale simulations, PBCs are imposed along the dislocation line direction to enforce a short, straight dislocation segment, whereas dislocations in experiments are usually much longer and curved.

In this paper, 0 K quenched dynamic CAC simulations with periodic energy minimisation are employed to study 3D sequential slip transfer across a Σ3 CTB in Cu and Al to render interface reactions that may be considered close to minimum energy pathways for thermally activated processes. A series of curved dislocations are nucleated from an FR source, which then move towards the CTB subject to a constant applied shear stress. Although the leading screw segment cuts into the twinned grain in Cu, it is absorbed and glides on the CTB in Al. In particular for Al,

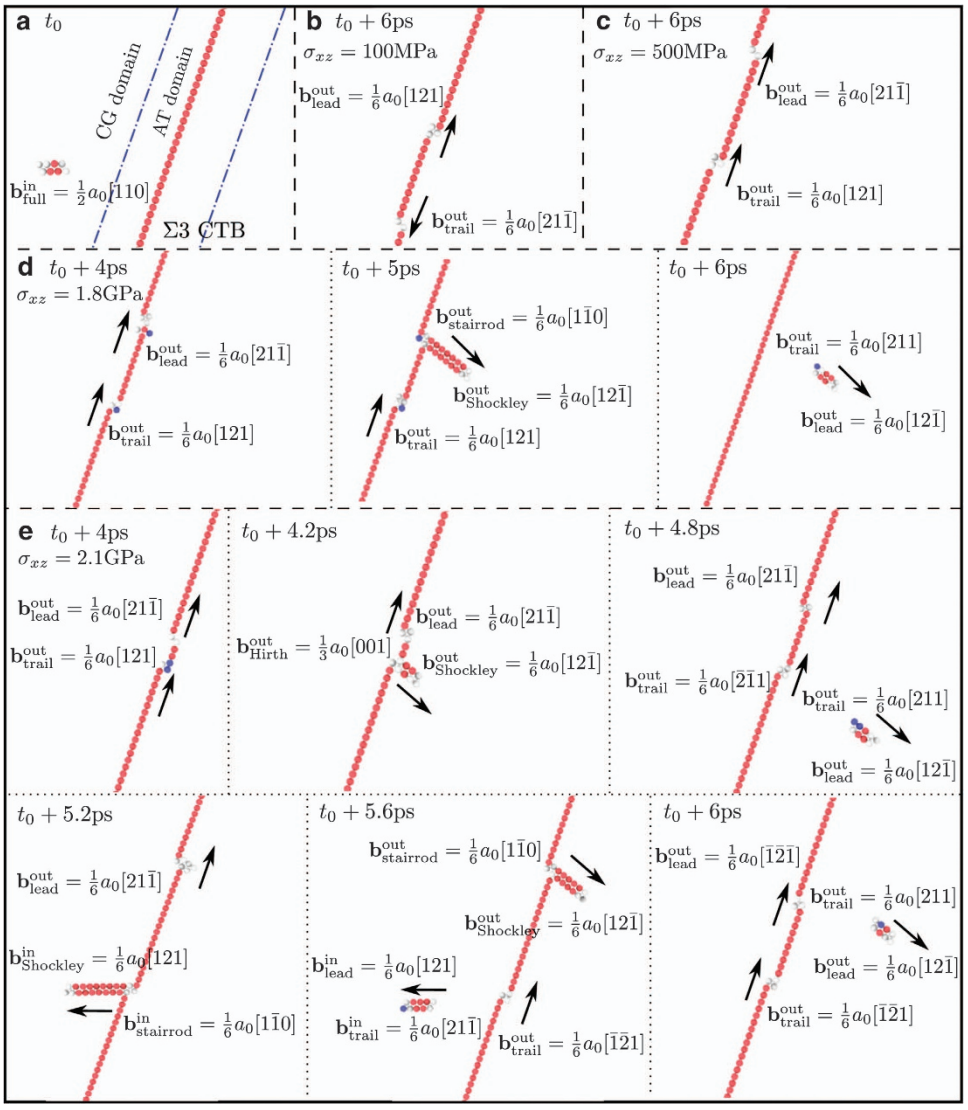

Figure 5. Snapshots of a straight screw dislocation interacting with a Σ3 CTB in a quasi 2D model for Al. Atoms are colored in the same manner as in Figure 2. The length of the dislocation line is reduced from 260*b* in Figure 1 to 26*b*. (**a**) Screw dislocation is in the coarse-grained domain; (**b**) at an applied stress of 100 MPa, the incoming dislocation splits into two Shockley partials, which then move in opposite directions; (**c**) at 500 MPa applied stress, the two CTB partial dislocations move in the same directions, leaving no CTB migration behind; (**d**) at 1.8 GPa applied stress, the incoming dislocation is first absorbed by the CTB then desorbed into the twinned grain, leaving behind a perfect boundary, similar to the NEB prediction for Cu;[10] (**e**) at the largest stress of 2.1 GPa, dislocations are desorbed into both incoming and outgoing grains.

four dislocation/CTB interaction modes are identified, which are affected by (1) applied shear stress, (2) dislocation line length, and (3) dislocation line curvature. Although we do not explicitly investigate the effect of the number of incoming dislocations, the effect of a dislocation pile-up can be manifested by varying the applied stress according to recent MD simulations.[17] In all cases studied in this paper, the dislocation/CTB reactions always follow the recombination-redissociation process, without forming any CTB dislocations in process of recombination. We emphasise that the results obtained for a single dislocation/GB interaction cannot be directly extrapolated to understand the practical case of slip transfer of dislocations in a pile-up in which the leading dislocation experiences a higher stress. The discrepancies between prior computational studies and experiments highlight the significance of the current work: it is important to directly model dislocation pile-ups, to let dislocations evolve freely in 3D, and to probe the mechanisms of slip transfer in polycrystalline and twinned metals using sufficiently large models. The slip transfer of more general dislocation types with different curvatures interacting with the Σ3 CTB, other GBs, and the influence of FR source exhaustion will be addressed in future work.

We note that these quasi-2D limitations are not confined to slip transfer processes. For example, there exists a characteristic length of a screw dislocation segment in BCC Fe above which more than one kink-pair can form which then strongly influences the dislocation mobility.[34] These observations suggest that 3D modeling using faithful interatomic potentials, though much less prevalent in the literature than quasi 2D simulations, is potentially of high utility in exploring more realistic dislocation behaviour. In this regard, the fully 3D CAC method opens a promising avenue to explore sequential slip transfer reactions, allowing the possibility for direct comparison of numerical simulations with quasi 4D (spatial correlation with time) characterisation of dislocations reconstructed from *in situ* TEM experiments.[8]

MATERIALS AND METHODS

For FCC Cu and Al, the EAM potentials of Mishin *et al.*[43,46] (with appropriate approximation in coarse-grained elements[30]) are employed because the evaluated stable and unstable stacking fault energies are close to experimentally measured values.[9] In the coarse-grained domain, 3D rhombohedral elements are employed with surfaces corresponding to {111} slip planes. Within each element, piecewise continuous first order shape and interpolation functions are employed. Between elements, neither displacement continuity nor interelement compatibility is required. We choose a uniform element size of 2197 atoms solved by first order Gaussian quadrature because it strikes a balance between high accuracy and high efficiency; approximations employed in CAC simulations have been explained and evaluated.[30] The lattice orientations are $x[110]$, $y[\bar{1}12]$, and $z[1\bar{1}1]$ in the incoming grain and $x[110]$, $y[\bar{5}\bar{5}2]$, and $z[1\bar{1}\bar{5}]$ in the outgoing grain, respectively. The domain around the FR source has full atomistic resolution because (1) the elements are of rhombohedral shape and (2) dislocation nucleation from a free surface can't be accurately described by the coarse-grained domain alone.[30] Similar to ref. 35 we find that the Lomer–Cottrell type sessile lock is either unstable or does not act as dislocation source in our model. The simulation cell size of the two materials differs only by their lattice parameter a_0, which is 3.615 Å for Cu and 4.05 Å for Al. The length along each direction in each grain is chosen by taking several factors into account: (1) curved dislocations should evolve freely in 3D—the box length along the x direction L_x for both grains needs to be large enough, e.g., $L_x = 66.3\,\text{nm} = 260b$ for Cu is sufficient to distinguish between quasi 2D and 3D[34] and allow dislocation segments to have a non-negligible curvature between stress-free surfaces, (2) the possible CTB dislocations need to migrate far from the initial site of dislocation/CTB interaction to minimise the back stress on subsequent slip transfer, so the box length along z direction for Cu is assigned as $L_z = 54.2\,\text{nm} = 213b$, which is larger than $196b$ used in a QC simulation;[26] (3) the outgoing dislocations should also be allowed to travel far from the interaction site on slip plane, so the outgoing grain length along y direction is selected for Cu as $L_y^{\text{out}} = 61.6\,\text{nm} = 242b$; (4) to minimise the image forces from the leftmost boundary, the incoming grain length along the y direction L_y^{in} is chosen to be 125.1 nm for Cu. As a result, the simulation cell contains 21,812 elements and about 9 million atoms, with 9,076,792 degrees of freedom in total compared with otherwise 56,823,260 in an equivalent full atomistic model. Our previous work shows that the coarse-graining efficiency of quasistatic CAC is about 20% higher than that estimated based on the number of degrees of freedom because the outer iteration in each energy minimisation step converges faster in the coarse-grained domain.[30] The dislocation density in the incoming grain containing one dislocation loop is about $2.95 \times 10^{14}/\text{m}^2$.

To account for both dislocation migration over relatively long distances and CTB structure evolution, we take a combined approach of quenched dynamic CAC accompanied by periodic quasistatic energy minimisation in the simulations. The quasistatic CAC[30] employs the conjugate gradient method to minimise energy at increments of applied loading; the convergence criterion corresponds to the ratio of absolute energy variation between successive iterations to the energy magnitude to lie below 10^{-6}. In quenched dynamic CAC, the atomic/nodal velocities are adjusted by atomic/equivalent nodal forces[30] following the 'quick-min' MD approach,[47] which, like dynamic CAC,[31] performs damped dynamics but without the damping term. Specifically, at each step in quenched dynamics, the velocity is projected in the direction of the force, with its component that is normal to the force discarded; then if the new velocity is antiparallel to the force, it is zeroed. The idea of quenched dynamics is to gradually drain energy by occasionally zeroing certain velocity components such that the system energy is forced towards a minimum at 0 K.[47] Employed in CAC for the first time, this is important in the current simulations since multiple dislocations are generated from FR sources at applied stress that progressively exceeds the critical stress, and then driven towards the CTB interface. As a result, the dislocated ensemble evolves away from equilibrium and periodic energy minimisation must therefore be regarded as a means of constrained optimisation for a sequence of nonequilibrium configurations. The quenched dynamics and quasistatic methods are shown to adequately avoid typical issues related to overdriven kinetics in dynamic simulations;[47] in particular, the 'quick-min' method is employed to find the minimum energy path in NEB calculations.[10] In this paper, we employ zero temperature CAC simulations to alleviate the finite temperature effect and focus on obtaining trajectories that are close to minimum energy pathways for evolution of structure during slip transfer because even MD cannot account for thermally activated processes that are important in explaining TEM results.[9] The Velocity Verlet algorithm is used to integrate the equation of motion, with a constant time step of 2 fs for both domains. Note that the time advancement in this paper is for quenched dynamics only. For all practical purposes, we regard the simulations to pertain to 0 K (or very nearly so) conditions.

In preparation for the simulations, we first compute the 0 K equilibrium structure of the CTB, which due to its simplicity can be achieved using energy minimisation without trying different in-plane translations.[1] A straight edge dislocation is introduced on the mid plane normal to z axis by moving atoms/nodes between two cylindrical holes by Burgers vector $b = \frac{1}{2}a_0[110]$, followed by energy minimisation. Only one dislocation segment is created to avoid the interaction between a dislocation dipole on parallel slip planes.[39] Once the equilibrium atomic configuration of the FR source is achieved, quenched dynamic CAC simulations are carried out with an increment of applied shear stress $\Delta\sigma_{xz} = 4$ MPa for each step until the shear stress reaches 1.2 GPa, which is then maintained using the PR method.[47] To prevent the simulation cell from rotating around the y axis, all nodes in the coarse-grained domain are constrained within the x–y plane, while the atoms are free to move to relax the stress free boundaries and obtain an energy minimised boundary structure. Note that while a large shear stress is necessary to bow out dislocations from the FR source and drive the dislocation pile-up towards the CTB, the high stress and accompanying inertia effect favour transmission over absorption.[9] Note that the quenched dynamic CAC still has some, albeit small, inertia effects because it is not strictly static minimisation. To alleviate inertia effects and accurately reproduce the CTB structure during dislocation impingement, the quasistatic CAC simulation (0 K energy minimisation) is performed every 500 steps before and every 100 steps after the first dislocation/CTB reaction. In the coarse-grained domain, the post-processing is performed after the atomic positions are interpolated from the nodal positions. Simulation results are visualised using Paraview[48] and OVITO;[49] the DXA[40] is also employed to identify dislocations and associated Burgers vector. Some runs are completed using Blacklight and Comet on Extreme Science and Engineering Discovery Environment (XSEDE).[50]

ACKNOWLEDGEMENTS

These results are based upon work supported by the National Science Foundation as a collaborative effort between Georgia Tech (CMMI-1232878) and University of Florida (CMMI-1233113). Any opinions, findings, and conclusions or recommendations expressed in this material are those of the authors and do not necessarily reflect the views of the National Science Foundation. The work of L.X. was supported in part by the Department of Energy, Office of Basic Energy Sciences under Award Number DE-SC0006539. The authors would like to thank Dr Zhaohui Jin, Dr Chaitanya Deo, Dr Josh Kacher, Dr Shreevant Tiwari, Dr Garritt Tucker, Dr Shengfeng Yang, Mr Matthew Priddy, Mr Zhi Zeng, and Mr Rui Che for helpful discussions, and Dr Alexander Stukowski for providing the dislocation extraction algorithm code. This work used the Extreme Science and Engineering Discovery Environment (XSEDE), which is supported by National Science Foundation grant number ACI-1053575.

CONTRIBUTIONS

D.L.M. and Y.C. conceived the research and provided guidance. S.X. performed computer simulations and wrote the paper. S.X. and L.X. developed the model and analysed the data. All authors discussed the results and revised the paper.

COMPETING INTERESTS

The authors declare no conflict of interest.

REFERENCES

1. Ramesh, K. T. *Nanomaterials: Mechanics and Mechanisms* (Springer, 2009).
2. Ratanaphan, S. *et al.* Grain boundary energies in body-centered cubic metals. *Acta Mater.* **88**, 346–354 (2015).
3. Counts, W. A., Braginsky, M. V., Battaile, C. C. & Holm, E. A. Predicting the Hall-Petch effect in fcc metals using non-local crystal plasticity. *Int. J. Plast.* **24**, 1243–1263 (2008).
4. Spearot, D. E. & Sangid, M. D. Insights on slip transmission at grain boundaries from atomistic simulations. *Curr. Opin. Solid State Mater. Sci.* **18**, 188–195 (2014).
5. Hirth, J. P. & Lothe, J. *Theory of Dislocations* (John Wiley & Sons, 1982).
6. Lee, T. C., Robertson, I. M. & Birnbaum, H. K. TEM in situ deformation study of the interaction of lattice dislocations with grain boundaries in metals. *Philos. Mag. A* **62**, 131–153 (1990).

7. Cottrell, A. H. in *Dislocations in Solids* Vol. 11 (eds Nabarro F. R. N. & Duesday M. S.) vii–xvii (Elsevier, 2002).
8. Kacher, J., Eftink, B. P., Cui, B. & Robertson, I. M. Dislocation interactions with grain boundaries. *Curr. Opin. Solid State Mater. Sci.* **18**, 227–243 (2014).
9. Chassagne, M., Legros, M. & Rodney, D. Atomic-scale simulation of screw dislocation/coherent twin boundary interaction in Al, Au, Cu and Ni. *Acta Mater.* **59**, 1456–1463 (2011).
10. Zhu, T., Li, J., Samanta, A., Kim, H. G. & Suresh, S. Interfacial plasticity governs strain rate sensitivity and ductility in nanostructured metals. *Proc. Natl Acad. Sci. USA* **104**, 3031–3036 (2007).
11. Zheng, Y. G., Lu, J., Zhang, H. W. & Chen, Z. Strengthening and toughening by interface-mediated slip transfer reaction in nanotwinned copper. *Scripta Mater.* **60**, 508–511 (2009).
12. Jin, Z. H. *et al.* The interaction mechanism of screw dislocations with coherent twin boundaries in different face-centred cubic metals. *Scripta Mater.* **54**, 1163–1168 (2006).
13. Jin, Z. H. *et al.* Interactions between non-screw lattice dislocations and coherent twin boundaries in face-centered cubic metals. *Acta Mater.* **56**, 1126–1135 (2008).
14. Ezaz, T., Sangid, M. D. & Sehitoglu, H. Energy barriers associated with slip-twin interactions. *Philos. Mag.* **91**, 1464–1488 (2011).
15. Szajewski, B. A. & Curtin, W. A. Analysis of spurious image forces in atomistic simulations of dislocations. *Model. Simul. Mater. Sci. Eng.* **23**, 025008 (2015).
16. Li, N. *et al.* Twinning dislocation multiplication at a coherent twin boundary. *Acta Mater.* **59**, 5989–5996 (2011).
17. Wang, J. Atomistic simulations of dislocation pileup: grain boundaries interaction. *JOM* **67**, 1515–1525 (2015).
18. de Koning, M., Miller, R., Bulatov, V. V. & Abraham, F. F. Modelling grain-boundary resistance in intergranular dislocation slip transmission. *Philos. Mag. A* **82**, 2511–2527 (2002).
19. Mayeur, J. R., Beyerlein, I. J., Bronkhorst, C. A. & Mourad, H. M. Incorporating interface affected zones into crystal plasticity. *Int. J. Plast.* **65**, 206–225 (2015).
20. Quek, S. S., Wu, Z., Zhang, Y. W. & Srolovitz, D. J. Polycrystal deformation in a discrete dislocation dynamics framework. *Acta Mater.* **75**, 92–105 (2014).
21. Puri, S., Acharya, A. & Rollett, A. Controlling plastic flow across grain boundaries in a continuum model. *Metall. Mater. Trans. A* **42**, 669–675 (2011).
22. Levitas, V. I. & Javanbakht, M. Phase transformations in nanograin materials under high pressure and plastic shear: nanoscale mechanisms. *Nanoscale* **6**, 162–166 (2014).
23. McDowell, D. L. A perspective on trends in multiscale plasticity. *Int. J. Plast* **26**, 1280–1309 (2010).
24. Liu, B. *et al.* Dislocation interactions and low-angle grain boundary strengthening. *Acta Mater.* **59**, 7125–7134 (2011).
25. McDowell, D. L. Viscoplasticity of heterogeneous metallic materials. *Mater. Sci. Eng. R Rep.* **62**, 67–123 (2008).
26. Shimokawa, T., Kinari, T. & Shintaku, S. Interaction mechanism between edge dislocations and asymmetrical tilt grain boundaries investigated via quasicontinuum simulations. *Phys. Rev. B* **75**, 144108 (2007).
27. Dewald, M. P. & Curtin, W. A. Multiscale modelling of dislocation/grain boundary interactions. II. Screw dislocations impinging on tilt boundaries in Al. *Philos. Mag.* **87**, 4615–4641 (2007).
28. Pavia, F. & Curtin, W. A. Parallel algorithm for multiscale atomistic/continuum simulations using LAMMPS. *Modelling Simul. Mater. Sci. Engl.* **23**, 055002 (2015).
29. Chen, Y. Reformulation of microscopic balance equations for multiscale materials modeling. *J. Chem. Phys.* **130**, 134706 (2009).
30. Xu, S., Che, R., Xiong, L., Chen, Y. & McDowell, D. L. A quasistatic implementation of the concurrent atomistic-continuum method for FCC crystals. *Int. J. Plast.* **72**, 91–126 (2015).
31. Xiong, L., Tucker, G., McDowell, D. L. & Chen, Y. Coarse-grained atomistic simulation of dislocations. *J. Mech. Phys. Solids* **59**, 160–177 (2011).
32. Xiong, L., Xu, S., McDowell, D. L. & Chen, Y. Concurrent atomistic-continuum simulations of dislocation-void interactions in fcc crystals. *Int. J. Plast.* **65**, 33–42 (2015).
33. Kashihara, K. & Inoko, F. Effect of piled-up dislocations on strain induced boundary migration (SIBM) in deformed aluminum bicrystals with originally Σ3 twin boundary. *Acta Mater.* **49**, 3051–3061 (2001).
34. Cai, W., Bulatov, V. V., Chang, J. P., Li, J. & Yip, S. in *Dislocations in Solids* Vol. 12 (eds Nabarro F. R. N. & Hirth J. P.) **64**, 1–80 (Elsevier, 2004).
35. Weinberger, C. R. & Tucker, G. J. Atomistic simulations of dislocation pinning points in pure face-centered-cubic nanopillars. *Model. Simul. Mater. Sci. Engl.* **20**, 075001 (2012).
36. Olmsted, D. L., Hardikar, K. Y. & Phillips, R. Lattice resistance and Peierls stress in finite size atomistic dislocation simulations. *Modelling Simul. Mater. Sci. Eng.* **9**, 215–247 (2001).
37. Chen, Z., Jin, Z. & Gao, H. Repulsive force between screw dislocation and coherent twin boundary in aluminum and copper. *Phys. Rev. B* **75**, 212104 (2007).
38. Scattergood, R. O. & Bacon, D. J. The strengthening effect of voids. *Acta Metall.* **30**, 1665–1677 (1982).
39. Shimokawa, T. & Kitada, S. Dislocation multiplication from the Frank-Read source in atomic models. *Mater. Trans.* **55**, 58–63 (2014).
40. Stukowski, A., Bulatov, V. V. & Arsenlis, A. Automated identification and indexing of dislocations in crystal interfaces. *Modelling Simul. Mater. Sci. Eng.* **20**, 085007 (2012).
41. Yang, Z. Q., Chisholm, M. F., He, L. L., Pennycook, S. J. & Ye, H. Q. Atomic-scale processes revealing dynamic twin boundary strengthening mechanisms in face-centered cubic materials. *Scripta Mater.* **67**, 911–914 (2012).
42. Jin, C., Xiang, Y. & Lu, G. Dislocation cross-slip mechanisms in aluminum. *Philos. Mag.* **91**, 4109–4125 (2011).
43. Mishin, Y., Farkas, D., Mehl, M. J. & Papaconstantopoulos, D. A. Interatomic potentials for monoatomic metals from experimental data and *ab initio* calculations. *Phys. Rev. B* **59**, 3393–3407 (1999).
44. Ercolessi, F. & Adams, J. B. Interatomic potentials from first-principles calculations: the force-matching method. *Europhys. Lett.* **26**, 583–588 (1994).
45. Wang, Y. M. *et al.* Defective twin boundaries in nanotwinned metals. *Nat. Mater.* **12**, 697–702 (2013).
46. Mishin, Y., Mehl, M. J., Papaconstantopoulos, D. A., Voter, A. F. & Kress, J. D. Structural stability and lattice defects in copper: *Ab initio*, tight-binding, and embedded-atom calculations. *Phys. Rev. B* **63**, 224106 (2001).
47. Tadmor, E. B. & Miller, R. E. *Modeling materials: continuum, atomistic and multiscale techniques* (Cambridge Univ. Press, 2011).
48. Schroeder, W., Martin, K. & Lorensen, B. *The Visualization Toolkit: An Object Oriented Approach to 3D Graphics* (Kitware, 2003).
49. Stukowski, A. Visualization and analysis of atomistic simulation data with OVITO --- the Open Visualization Tool. *Modelling Simul. Mater. Sci. Eng.* **18**, 015012 (2010).
50. Towns, J. *et al.* XSEDE: Accelerating scientific discovery. *Comput. Sci. Eng.* **16**, 62–74 (2014).